MICROBIOTA

Helminth infection promotes colonization resistance via type 2 immunity

Deepshika Ramanan,[1,2]* Rowann Bowcutt,[3]* Soo Ching Lee,[4] Mei San Tang,[3] Zachary D. Kurtz,[2,3] Yi Ding,[5] Kenya Honda,[6,7] William C. Gause,[8] Martin J. Blaser,[3] Richard A. Bonneau,[9,10,11] Yvonne A.L. Lim,[4]† P'ng Loke,[3]†‡ Ken Cadwell[1,3]†‡

Increasing incidence of inflammatory bowel diseases, such as Crohn's disease, in developed nations is associated with changes to the microbial environment, such as decreased prevalence of helminth colonization and alterations to the gut microbiota. We find that helminth infection protects mice deficient in the Crohn's disease susceptibility gene *Nod2* from intestinal abnormalities by inhibiting colonization by an inflammatory *Bacteroides* species. Resistance to *Bacteroides* colonization was dependent on type 2 immunity, which promoted the establishment of a protective microbiota enriched in Clostridiales. Additionally, we show that individuals from helminth-endemic regions harbor a similar protective microbiota and that deworming treatment reduced levels of Clostridiales and increased Bacteroidales. These results support a model of the hygiene hypothesis in which certain individuals are genetically susceptible to the consequences of a changing microbial environment.

Dramatic increases in the incidence of inflammatory bowel disease (IBD) in the developed world point toward alterations in the microbial environment, including changes to the gut microbiota (*1*) and decreased exposure to intestinal parasites such as helminths (*2*). Evidence supporting a central role of the microbiota in the pathogenesis of IBD has led to a growing interest in defining the symbiotic relationship between the host and specific microbial species (*3*). In insects, symbiotic relationships can develop to defend against environmental hazards (defensive symbiosis) (*4*); this concept may be applicable to host-microbiota interactions. For example, specific bacterial taxa found within the human gut microbiota probably mediate resistance to antibiotic-associated diarrhea caused by *Clostridium difficile* (*5*). The loss of beneficial members of the microbiota potentially contributes to chronic inflammatory diseases. Additionally, helminths and the gut microbiota have coevolved with their mammalian

[1]Kimmel Center for Biology and Medicine at the Skirball Institute, New York University School of Medicine, New York, NY 10016, USA. [2]Sackler Institute of Graduate Biomedical Sciences, New York University School of Medicine, New York, NY 10016, USA. [3]Departments of Microbiology and Medicine, New York University School of Medicine, New York, NY 10016, USA. [4]Department of Parasitology, Faculty of Medicine, University of Malaya, Kuala Lumpur, Malaysia. [5]Department of Pathology, New York University Langone Medical Center, New York, NY 10016, USA. [6]RIKEN Center for Integrative Medical Sciences (IMS), Yokohama, Kanagawa 230-0045, Japan. [7]Japan Agency for Medical Research and Development (AMED)–Core Research for Evolutional Science and Technology (CREST), Tokyo 100-0004, Japan. [8]Center for Immunity and Inflammation, New Jersey Medical School, Rutgers, The State University of New Jersey, Newark, NJ 07101, USA. [9]Department of Biology, Center for Genomics and Systems Biology, New York University, New York, NY 10003, USA. [10]Courant Institute of Mathematical Sciences, New York University, New York, NY 10012, USA. [11]Simons Center for Data Analysis, Simons Foundation, New York, NY 10011, USA.
*These authors contributed equally to this work. **†Corresponding author. Email: ken.cadwell@med.nyu.edu (K.C.); png.loke@nyumc.org (P.L.); limailian@um.edu.my (Y.A.L.L.)**
‡These authors contributed equally equally to this work.

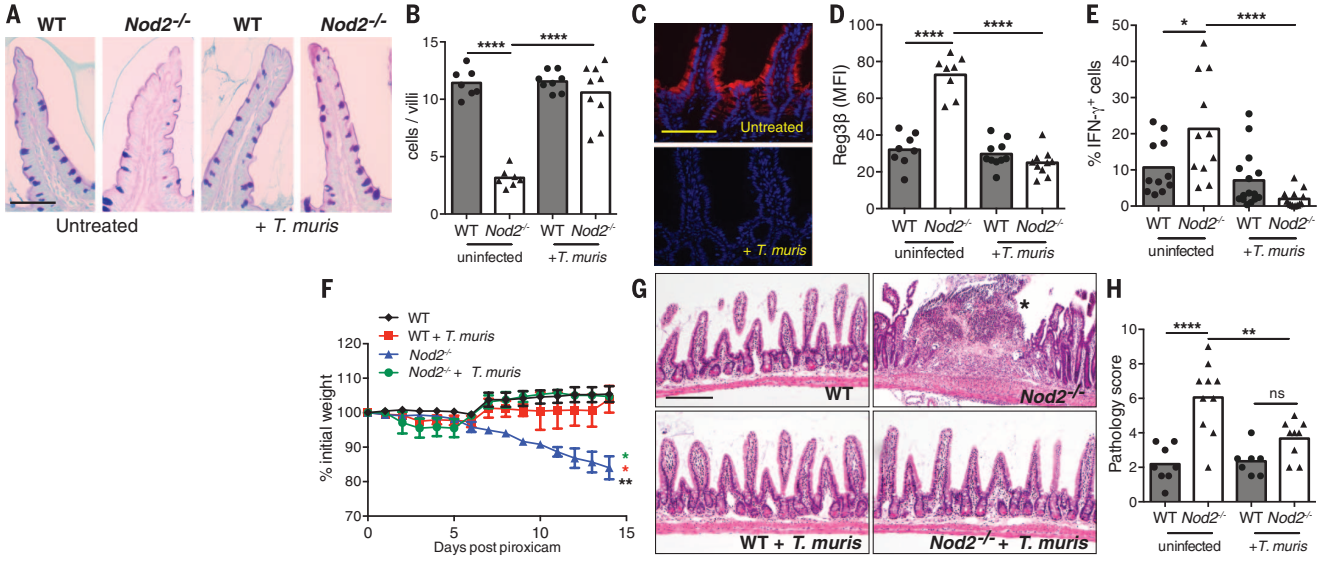

Fig. 1. *Trichuris muris* infection reverses intestinal abnormalities in *Nod2*$^{-/-}$ mice. (**A** and **B**) SI sections stained with PAS (periodic acid–Schiff)–Alcian blue (A) and quantification of the number of goblet cells displaying normal morphology per villi (B) from uninfected and *T. muris*–infected WT and *Nod2*$^{-/-}$ mice ($n \geq 7$ per genotype). (**C** and **D**) Immunofluorescence (IF) analysis of Reg3β in the small intestine (C) and quantification of the mean fluorescence intensity (D) of the aforementioned mice ($n \geq 8$ per genotype). (**E**) Quantification of the proportion of CD8$^+$ IELs expressing IFN-γ by flow cytometry ($n \geq 11$ per genotype). (**F** to **H**) Quantification of weight loss (F), SI sections stained with hematoxylin and eosin (G), and quantification of pathology (*19*) (H) after piroxicam treatment of uninfected and *T. muris*–infected WT and *Nod2*$^{-/-}$ mice. The asterisk in (G) denotes an abscess ($n \geq 7$ per genotype). *$P <$ 0.05; **$P < 0.01$; ****$P < 0.0001$ by analysis of variance (ANOVA), with Holm-Sidak multiple comparisons test for (B), (D) to (F), and (H). ns, not significant. Scale bars represent 50 μm in (A) and 100 μm in (C) and (G). Data are represented in (F) as mean ± SEM (error bars) from at least two independent experiments. In (B), (D), (E), and (H), each data point represents an individual mouse, and each horizontal bar denotes a mean value (at least two independent experiments).

hosts, but the mechanisms of these interactions and the consequence of decreased exposure to intestinal helminths remain unclear. We find that helminths can reduce intestinal inflammatory responses by promoting expansion of protective bacterial communities that inhibit proinflammatory bacterial taxa.

We previously reported that mice deficient in *Nod2* develop several small intestinal (SI) abnormalities, in a manner dependent on a ubiquitous member of the gut microbiota, *Bacteroides vulgatus* (*6*). Consistent with the specific association between human *NOD2* variants and ileal Crohn's disease (*7*), an IBD that affects the small intestine, the most notable abnormality was a SI goblet cell defect that resulted in a compromised mucus layer, allowing sustained colonization by *B. vulgatus*. We found that chronic infection of *Nod2*$^{-/-}$ mice with the parasitic worm *Trichuris muris* restored SI goblet cell numbers and morphology (Fig. 1, A and B, and fig. S1, A and B). These changes were not detected in the colon, and wild-type (WT) mice infected with *T. muris* did not display nonspecific goblet cell hyperplasia (fig. S1C). Elevated epithelial levels of the antimicrobial lectin Reg3β and interferon-γ$^+$ (IFN-γ$^+$) CD8$^+$ intraepithelial lymphocytes (IELs), inflammatory markers associated with goblet cell defects in *Nod2*$^{-/-}$ mice (*6*), were also reduced upon *T. muris* infection (Fig. 1, C to E; and figs. S1, D and E, and S2). *Nod2*$^{-/-}$ mice develop severe intestinal pathologies after SI injury induced by the nonsteroidal anti-inflammatory drug piroxicam. Infection with *T. muris* prevented the intestinal bleeding and perforation, exaggerated weight loss, mucus depletion, splenomegaly, and bacterial translocation observed in uninfected *Nod2*$^{-/-}$ mice treated with piroxicam (Fig. 1F and figs. S3, A to C, and S4). Blind histology analysis confirmed reductions in specific pathologies such as abscesses, epithelial hyperplasia, villus blunting, and immune infiltrates (Fig. 1, G and H, and fig. S3, D to J). These results indicate that *T. muris* infection ameliorates spontaneous and inducible intestinal defects in *Nod2*$^{-/-}$ mice.

Consistent with the dependence of these inflammatory pathologies on *B. vulgatus* (*6*), infection with *T. muris* reduced the bacterial burden to the limit of detection in the stool and SI tissue of *Nod2*$^{-/-}$ mice (Fig. 2, A and F). *B. vulgatus* inhibition was dependent on lymphocytes (fig. S5, A to C), potentially reflecting goblet cell activation by type 2 cytokines [interleukin-4 (IL-4) and IL-13] produced by T helper (T_H) cells during helminth infections. We found increased phosphorylation of the type 2 transcription factor Stat6 in the SI epithelium of *T. muris*–infected *Nod2*$^{-/-}$ mice (Fig. 2B and fig. S5D). Additionally, *T. muris* infection inhibited *B. vulgatus* only transiently and did not restore goblet cells in *Stat6*$^{-/-}$ mice reconstituted with *Nod2*$^{-/-}$ bone marrow (Fig. 2C and fig. S5E). *Nod2*$^{-/-}$ mice infected with *T. muris* displayed a dominant T_H2 response characterized by a >10-fold increase in IL-13$^+$ CD4$^+$ T cells in the lamina propria (Fig. 2, D and E, and fig. S5, F and G). We confirmed these results with a second helminth, *Heligmosomoides polygyrus*, which induced an even greater T_H2 response compared with *T. muris*, perhaps reflecting the distinct anatomical niches of these parasites (Fig. 2, H and D, and figs. S6, C and D, and S7B). *H. polygyrus* completely abolished tissue-associated *B. vulgatus*, restored goblet cells, and reduced IFN-γ$^+$ IELs in *Nod2*$^{-/-}$ mice (Fig. 2, F and G, and figs. S6, A and B, and S7A). Blockade of IL-13 inhibited the effect of *H. polygyrus* on *B. vulgatus* and goblet cells, and administration of recombinant IL-13 (rIL-13) or rIL-4 to *Nod2*$^{-/-}$ mice was sufficient to reproduce the effect of helminth infection (Fig. 2, I to L, and

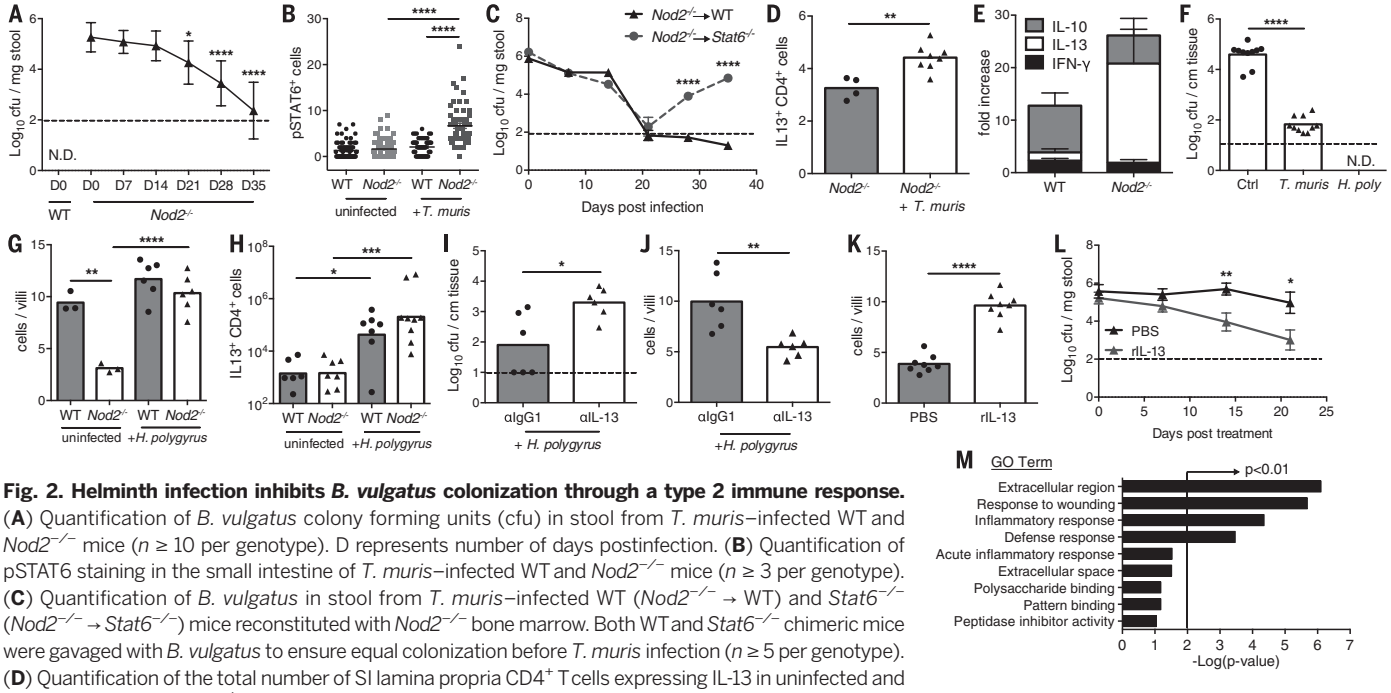

Fig. 2. Helminth infection inhibits *B. vulgatus* colonization through a type 2 immune response. (**A**) Quantification of *B. vulgatus* colony forming units (cfu) in stool from *T. muris*–infected WT and *Nod2*$^{-/-}$ mice ($n \geq 10$ per genotype). D represents number of days postinfection. (**B**) Quantification of pSTAT6 staining in the small intestine of *T. muris*–infected WT and *Nod2*$^{-/-}$ mice ($n \geq 3$ per genotype). (**C**) Quantification of *B. vulgatus* in stool from *T. muris*–infected WT (*Nod2*$^{-/-}$ → WT) and *Stat6*$^{-/-}$ (*Nod2*$^{-/-}$ → *Stat6*$^{-/-}$) mice reconstituted with *Nod2*$^{-/-}$ bone marrow. Both WT and *Stat6*$^{-/-}$ chimeric mice were gavaged with *B. vulgatus* to ensure equal colonization before *T. muris* infection ($n \geq 5$ per genotype). (**D**) Quantification of the total number of SI lamina propria CD4$^+$ T cells expressing IL-13 in uninfected and *T. muris*–infected *Nod2*$^{-/-}$ mice ($n \geq 4$ per genotype). (**E**) Fold increase in the number of CD4$^+$ T cells producing IFN-γ, IL-13, or IL-10 in the SI lamina propria of *T. muris*–infected WT and *Nod2*$^{-/-}$ mice, normalized to uninfected mice ($n \geq 4$ per genotype). (**F**) Quantification of *B. vulgatus* associated with SI tissue of uninfected, *T. muris*–infected, and *H. polygyrus*–infected *Nod2*$^{-/-}$ mice ($n \geq 10$ per genotype). (**G** and **H**) Quantification of goblet cells displaying normal morphology per villi (G) and total number of SI lamina propria CD4$^+$ T cells expressing IL-13 (H) in uninfected and *H. polygyrus*–infected WT and *Nod2*$^{-/-}$ mice ($n \geq 3$ per genotype). (**I** and **J**) Quantification of *B. vulgatus* in SI tissue (I), and goblet cells displaying normal morphology (J) in *H. polygyrus*–infected *Nod2*$^{-/-}$ mice treated with antibody to IL-13 or isotype control ($n = 6$ per genotype). (**K** and **L**) Quantification of goblet cells displaying normal morphology (K) and *B. vulgatus* in stool (L) in *Nod2*$^{-/-}$ mice treated with recombinant IL-13 or phosphate-buffered saline (PBS) ($n = 8$ per genotype). (**M**) Pathway analysis based on Gene Ontology (GO) terms of genes up-regulated in *Nod2*$^{-/-}$ mice treated with recombinant IL-13 compared with PBS controls. *$P < 0.05$; **$P < 0.01$; ***$P < 0.001$; ****$P < 0.0001$ by ANOVA, with Holm-Sidak multiple comparisons test for (A), (B), (G) and (H) and unpaired *t* test for (C), (D), (F), and (I) to (L). N.D., not detected. Data in (A), (B), (C), (E), and (L) are represented as mean ± SEM (error bars) from at least two independent experiments. In (D) and (F) to (K), each data point represents an individual mouse, and each bar denotes a mean value [at least two independent experiments, excluding the generation of bone marrow chimeras in (C)].

fig. S6E). RNA sequencing (RNA-seq) analysis of intestinal tissues from rIL-13–treated *Nod2*$^{-/-}$ mice revealed a wound-healing response characterized by expression of M2 macrophage genes (Fig. 2M, fig. S6F, and table S1). These results are consistent with the anti-inflammatory role of M2 macrophages in the gut (*8*, *9*) and help to explain how helminth infection ameliorates the exacerbated intestinal injury response in *Nod2*$^{-/-}$ mice. These results do not contradict the regulatory response induced by *H. polygyrus* in the colon (*9*, *10*), because type 2 immunity and regulatory T cells can function concurrently to reduce inflammation (*11*).

The reduction of *B. vulgatus* in the presence of helminths could be mediated indirectly through alterations to the gut microbiota downstream of the type 2 response. Cohousing mice allows for coprophagic transmission of microbial populations without transfer of parasites, because the worms are not sexually mature until ~35 days postinfection and eggs require several weeks for germination (*12*). We found that uninfected *Nod2*$^{-/-}$ mice cohoused with *T. muris*–infected *Nod2*$^{-/-}$ mice showed a similar decrease in *B. vulgatus* colonization (Fig. 3A and fig. S8A). This reduction in *B. vulgatus* levels was not observed in uninfected *Nod2*$^{-/-}$ mice when they were instead cohoused with *T. muris*–infected WT mice (fig. S8, B and C). 16*S* ribosomal DNA sequencing analysis of stool samples indicated that the alterations to microbial community compositions are different for *T. muris*–infected WT and *Nod2*$^{-/-}$ mice (Fig. 3B), which may reflect different intestinal responses between WT and *Nod2*$^{-/-}$ mice (Fig. 2E). Whereas infected WT mice have reduced alpha diversity, as previously reported (*13*, *14*), *Nod2*$^{-/-}$ mice increased their alpha diversity at day 21 postinfection (fig. S8D). The most significantly reduced bacterial taxa in infected *Nod2*$^{-/-}$ mice were the *Prevotella* and *Bacteroides* genera (belonging to the order Bacteroidales), and the Lachnospiraceae family of the order Clostridiales was the most significantly increased (Fig. 3C). The increase in Clostridiales was less evident in WT mice (Fig. 3B), which potentially explains why cohousing *Nod2*$^{-/-}$ mice with *T. muris*–infected WT mice was not effective in reducing the *B. vulgatus* burden. The expansion of Clostridiales was also observed in the stool of uninfected *Nod2*$^{-/-}$ mice treated with rIL-13 or rIL-4 (Fig. 3D and fig. S8E). The expansion of Clostridiales was even more pronounced among tissue-associated bacteria in the small intestine after infection with *T. muris* or *H. polygyrus* (fig. S8, F and G). Thus, helminth infection and type 2 cytokines inhibit *B. vulgatus* and expand Clostridiales strains.

To determine whether Clostridia can directly inhibit *B. vulgatus*, we inoculated *Nod2*$^{-/-}$ mice with a mixture of *Clostridium* clusters IV, XIVa, and XVIII and Erysipelotrichales strains isolated from human feces (*15*). Repetitive gavaging of *Nod2*$^{-/-}$ mice with this mixture, but not sterile broth or an equivalent number of *Lactobacillus johnsonii* [a host-interactive commensal bacterium (*16*)], led to a decrease in *B. vulgatus* colonization over time (Fig. 3E). The addition of mucin to anaerobic cultures accelerates the growth of all three representative Clostridia strains tested, but not *B. vulgatus* (Fig. 3, F and G, and fig. S8, H and I), which suggests that increased mucus production by goblet cells may alter the intestinal environment to favor Clostridiales. Hence, our results indicate that in *Nod2*$^{-/-}$ mice, the mucus response associated with type 2 immunity during helminth infection expands Clostridia strains that can inhibit colonization of *B. vulgatus*.

Inflammatory bowel disease is less prevalent in regions where helminth colonization is endemic. We previously found that helminth-colonized individuals among indigenous populations in Malaysia, known as the Orang Asli, have higher microbial diversity than helminth-negative individuals (*17*). We compared individuals living in urbanized Kuala Lumpur with rural Orang Asli of the Temuan subtribe from a village 40 km away (5.3% versus 96% of individuals colonized by intestinal helminths, respectively) (table S2). People living in Kuala Lumpur predominantly cluster in a group driven by the abundance of a single *Bacteroides* operational taxonomic unit (OTU) (TaxID 3600504), which is less widespread in the Orang Asli (Fig. 4, A and B). In contrast, the helminth-positive Orang Asli people fall into

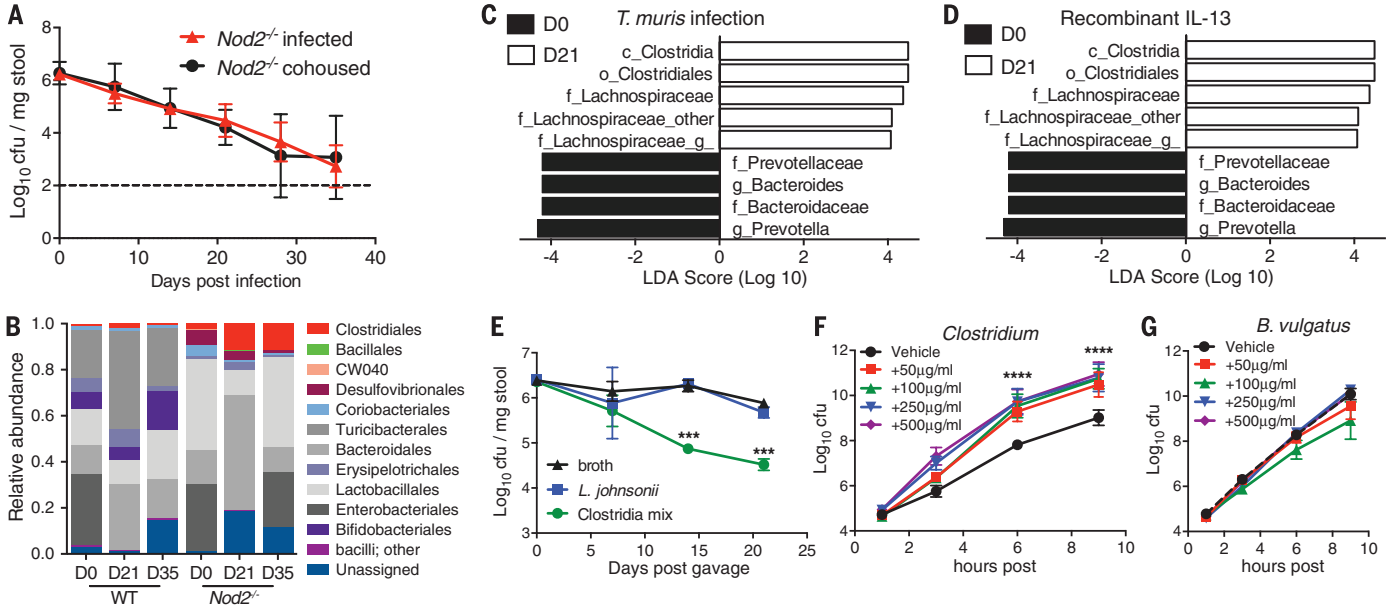

Fig. 3. Inhibition of *B. vulgatus* is associated with expansion of Clostridiales after helminth infection. (**A**) Quantification of *B. vulgatus* in stool harvested from uninfected and *T. muris*–infected *Nod2*$^{-/-}$ mice cohoused for the duration of the experiment ($n \geq 4$). (**B**) Relative abundance of taxonomic groups in response to *T. muris* infection in the stool of WT and *Nod2*$^{-/-}$ mice, as determined by 16*S* sequencing ($n \geq 5$ per genotype). (**C**) Supervised analysis of 16*S* sequencing data with LDA effect size (LEfSe), comparing *Nod2*$^{-/-}$ mice at D0 and D21 postinfection with *T. muris* using an LDA threshold score of 4 ($n \geq 5$). (**D**) LEfSE analysis to determine alterations to the stool microbiota after recombinant IL-13 treatment of *Nod2*$^{-/-}$ mice using an LDA threshold score of 4 ($n \geq 5$). (**E**) Quantification of *B. vulgatus* in stool harvested from *Nod2*$^{-/-}$ mice gavaged with sterile broth, *L. johnsonii*, or a mix of 17 Clostridiales and Erysipelotrichales strains ($n \geq 3$). (**F** and **G**) Quantification of *Clostridium* species (Clostridiales 28) (F) or *B. vulgatus* (G) in the presence of varying concentrations of pig intestinal mucin or vehicle in the culture media. ***$P <$ 0.001; ****$P < 0.0001$ by ANOVA, with Holm-Sidak multiple comparisons test for (E) and (F). Data are represented as mean ± SEM (error bars) from at least two independent experiments.

a second group characterized by *Faecalibacterium* and *Prevotella* (Fig. 4A). This division between the microbiota dominance of urban and rural populations is also observed in other Asian countries (*18*).

To control for factors other than helminth colonization (e.g., diet), we analyzed stool samples collected from the Orang Asli before and after deworming treatment with albendazole (fig. S9, A and B, and table S3). Alpha diversity of microbial communities was significantly reduced after treatment (Fig. 4F and fig. S9, C and D). We used the linear discriminant analysis (LDA) effect size (LEfSe) algorithm to show that Clostridiales was the most significantly reduced order, whereas Bacteroidales (*Prevotella*) was significantly expanded after treatment (Fig. 4, C to E, and fig. S9E). Using the egg-burden data, we combined centered log-ratio transformation with partial least squares regression to examine within-subject changes, incorporating a repeated measures design (*19*). The resulting model showed that posttreatment intraindividual changes in *Trichuris trichiura* egg burden are strongly associated with a small set of bacterial taxa, independent of age and gender (Fig. 4G; fig. S10, A to C; and table S4). Specifically, *Dialister* and *Coprococcus* are two members of the order Clostridiales that are positively associated with changes in egg burden, whereas the Bacteroidales species *Prevotella* and another OTU are negatively associated (Fig. 4H and fig. S10D). Individuals without reduced egg burden did not show these microbiome changes, indicating that these findings are unlikely to be due to nonspecific effects of albendazole treatment (fig. S10, E to G). Overall, these data support our hypothesis that helminth infection promotes the expansion of Clostridiales communities that outcompete Bacteroidales communities, although we did not examine the T_H2 response. Finally, we applied a method [sparse inverse covariance estimation for ecological association inference (SPIEC-EASI)] for inference of microbial ecological networks (*20*) to publicly available human microbiome data sets consisting of healthy U.S. residents (Human Microbiome Project and American Gut Project) and pediatric IBD patients (RISK cohort) (*21*–*23*) and found that the antagonistic relationship between Clostridiales and Bacteroidales is the most consistently observed negative relationship (Fig. 4, I and J, and fig. S11).

In this study, Clostridiales are an example of defensive symbionts that display an antagonistic interaction with another common commensal bacteria (Bacteroidales), which we consistently observed in all human gut microbiome data sets. Bacteroidales are pathogenic only in susceptible *Nod2*-deficient hosts, and this competition reverses disease pathologies. Many Crohn's disease patients do not carry *NOD2* variants and, hence, may not respond to helminths, which have failed in clinical trials. Helminths may be beneficial

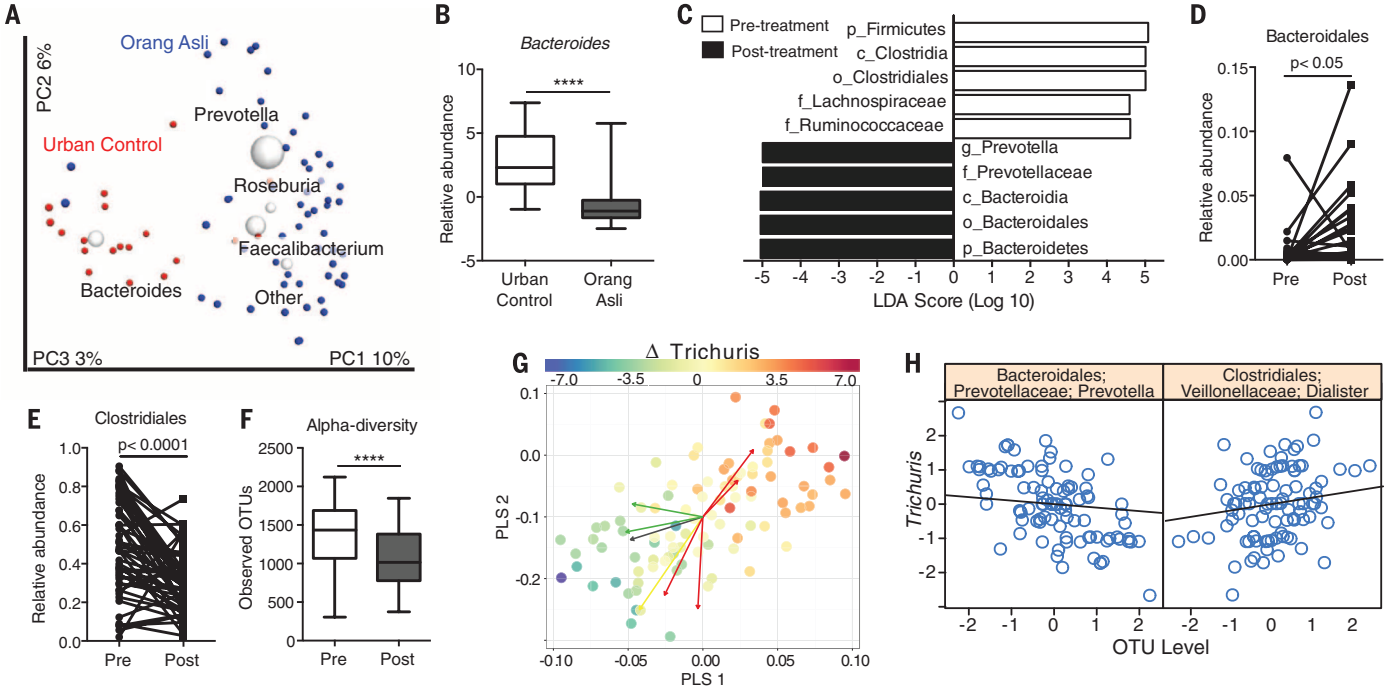

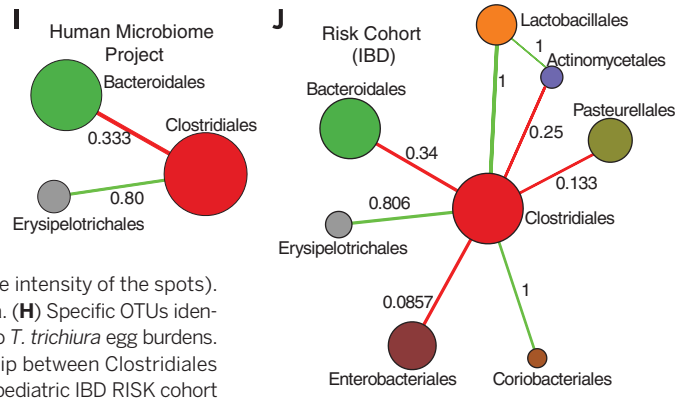

Fig. 4. Helminth colonization in humans is associated with a decrease in Bacteroidales and an increase in Clostridiales levels. (**A**) Beta diversity plots of gut microbiota from urban controls in Kuala Lumpur (red dots) and the Orang Asli (blue dots). (**B**) Relative abundance of a dominant *Bacteroides* OTU in the Orang Asli and urban controls. (**C** to **F**) Supervised LEfSE analysis (C), relative abundance of Bacteroidales (D) and Clostridiales (E), and alpha diversity as observed OTUs (F) of the Orang Asli stool microbiota before and after treatment with albendazole (n = 19 for urban controls and 55 Orang Asli; n = 53 for deworming experiments). (**G**) Partial least squares regression biplots examining within-subject variances with repeated measures design to identify bacterial taxa associated with *T. trichiura* worm burden (illustrated by the intensity of the spots). Red arrows represent Clostridiales taxa; green arrows denote Bacteroidales taxa. (**H**) Specific OTUs identified to be positively (*Dialister*) or negatively (*Prevotella*) associated with changes to *T. trichiura* egg burdens. (**I** and **J**) Microbial network inference demonstrating an antagonistic relationship between Clostridiales and Bacteroidales communities from the Human Microbiome Project (I) and the pediatric IBD RISK cohort (J). The node diameter is proportional to the geometric mean of the OTU's relative abundance. Numerical values on the edges represent the fraction of edges that are either majority-positive (green) or majority-negative (red). Also see fig. S10. ****P < 0.0001 by unpaired t test in (B) and paired t test in (D) to (F).

only in patients with *NOD2* variants or proinflammatory *Bacteroidales* species. We propose that certain individuals may be more susceptible to deleterious consequences of a changing microbial environment, and an understanding of the contribution of genetic and environmental factors toward the development of inflammatory diseases is essential to devise therapeutic strategies that consider the heterogeneity of etiologies.

REFERENCES AND NOTES

1. Y. Belkaid, T. W. Hand, *Cell* **157**, 121–141 (2014).
2. J. V. Weinstock, D. E. Elliott, *Inflamm. Bowel Dis.* **15**, 128–133 (2009).
3. N. Kamada, G. Núñez, *Gastroenterology* **146**, 1477–1488 (2014).
4. J. Jaenike, R. Unckless, S. N. Cockburn, L. M. Boelio, S. J. Perlman, *Science* **329**, 212–215 (2010).
5. C. G. Buffie *et al*., *Nature* **517**, 205–208 (2015).
6. D. Ramanan, M. S. Tang, R. Bowcutt, P. Loke, K. Cadwell, *Immunity* **41**, 311–324 (2014).
7. I. Cleynen *et al*., *Lancet* **387**, 156–167 (2016).
8. M. M. Hunter *et al*., *Gastroenterology* **138**, 1395–1405 (2010).
9. T. Ziegler *et al*., *J. Immunol.* **194**, 1555–1564 (2015).
10. L. Hang *et al*., *J. Immunol.* **191**, 1927–1934 (2013).
11. M. M. Zaiss *et al*., *Immunity* **43**, 998–1010 (2015).
12. J. E. Klementowicz, M. A. Travis, R. K. Grencis, *Semin. Immunopathol.* **34**, 815–828 (2012).
13. J. B. Holm *et al*., *PLOS ONE* **10**, e0125495 (2015).
14. A. Houlden *et al*., *PLOS ONE* **10**, e0125945 (2015).
15. K. Atarashi *et al*., *Nature* **500**, 232–236 (2013).
16. R. D. Pridmore *et al*., *Proc. Natl. Acad. Sci. U.S.A.* **101**, 2512–2517 (2004).
17. S. C. Lee *et al*., *PLOS Negl. Trop. Dis.* **8**, e2880 (2014).
18. J. Nakayama *et al*., *Sci. Rep.* **5**, 8397 (2015).
19. Materials and methods are available as supplementary materials on *Science* Online.
20. Z. D. Kurtz *et al*., *PLOS Comput. Biol.* **11**, e1004226 (2015).
21. D. Gevers *et al*., *Cell Host Microbe* **15**, 382–392 (2014).
22. D. Gevers *et al*., *PLOS Biol.* **10**, e1001377 (2012).
23. "Preliminary characterization of the american Gut population" (Technical Report, American Gut Project, 2014); www.microbio.me/AmericanGut/static/img/mod1_main.pdf.

ACKNOWLEDGMENTS

We thank D. Artis for seed stock of *T. muris*, H. Silva for assistance with flow cytometry panels, B. Zeck and L. Chiriboga for assistance with immunohistochemistry, and New York University School of Medicine Flow Cytometry and Cell Sorting Center, Genomics Core, and Immunohistochemistry Core (supported in part by NIH grants P30CA016087 and UL1 TR00038). The data presented in this manuscript are tabulated in the main paper and in the supplementary materials. RNA-seq data have been made publicly available and can be accessed using the Gene Expression Omnibus accession number GSE76504. Fastq files and corresponding mapping files for 16*S* sequencing data are available on request. Clostridia strains derived from human microbiota are available from K.H. under a material transfer agreement with RIKEN. K.H. is an inventor on patent applications (U.S. 14/362,097, PCT/JP2012/007687) filed by the University of Tokyo, related to the human-derived Clostridia, and is a scientific adviser to Vedanta Biosciences. P.L., K.C., D.R., and R.B. are inventors on a patent application filed by New York University, related to the studies reported here. This work was supported by NIH grants DK103788 (K.C. and P.L.), DK093668 (K.C.), HL123340 (K.C.), AI093811 (P.L.), AI007180 (Z.D.K. and M.J.B.), DK090989 (Z.D.K. and M.J.B.), and AI107588 (W.C.G.); the Broad Medical Research Program (P.L.); the Kevin and Marsha Keating Family Foundation (P.L.); The MCJ Amelior Foundation (W.C.G.); NIH National Center for Advancing Translational Sciences grant UL1 TR000038 (K.C. and P.L.); a philanthropic contribution from B. Levine (K.C. and P.L.); and University of Malaya–Ministry of Education HIR grant UM.C/625/HIR/MOE/MED/23 (Y.A.L.L. and P.L.). K.C. is a Burroughs Wellcome Fund Investigator in the Pathogenesis of Infectious Diseases.

SUPPLEMENTARY MATERIALS

www.sciencemag.org/content/352/6285/608/suppl/DC1
Materials and Methods
Figs. S1 to S11
Table S1 to S4
References (*24*–*48*)

25 August 2015; accepted 21 March 2016
Published online 14 April 2016
10.1126/science.aaf3229

Helminth infection promotes colonization resistance via type 2 immunity

Deepshika Ramanan, Rowann Bowcutt, Soo Ching Lee, Mei San Tang, Zachary D. Kurtz, Yi Ding, Kenya Honda, William C. Gause, Martin J. Blaser, Richard A. Bonneau, Yvonne A.L. Lim, P'ng Loke and Ken Cadwell

Science **352** (6285), 608-612.
DOI: 10.1126/science.aaf3229originally published online April 14, 2016

Parasitic worms affect gut microbes

Improved hygiene practices in high-income countries may come with an increased risk of developing inflammatory bowel disease (IBD) or other similar disorders. Ramanan *et al.* show that intestinal helminth infection, caused by parasitic worms, protects IBD-susceptible mice from developing the disease. The infection increases specific protective species and limits other inflammatory members of the microbiota. People from helminth-endemic regions harbored a similar protective microbiota, and their deworming led to an increase in inflammatory Bacteroidales species, similar to what the authors observed in the mice. Thus, a changing microbial environment may shape susceptibility to inflammatory disease.

Science, this issue p. 608